Plasmonic band edge effects on the transmission properties of metal gratings

D. de Ceglia,[1,a] M. A. Vincenti,[1] M. Scalora,[2] N. Akozbek,[2] and M. J. Bloemer[2]

[1]*AEgis Technologies Inc., 410 Jan Davis Dr, Huntsville – AL, 35806, USA*
[2]*Charles M. Bowden Research Center, AMSRD-AMR-WS-ST, Redstone Arsenal, Huntsville, AL 35898, USA*

(Received 10 March 2011; accepted 10 August 2011; published online 1 September 2011)

We present a detailed analysis of the optical properties of one-dimensional arrays of slits in metal films. Although enhanced transmission windows are dominated by Fabry-Perot cavity modes localized inside the slits, the periodicity introduces surface modes that can either enhance or inhibit light transmission. We thus illustrate the interaction between cavity modes and surface modes in both finite and infinite arrays of slits. In particular we study a grating that clearly separates surface plasmon effects from Wood-Rayleigh anomalies. The periodicity of the grating induces a strong plasmonic band gap that inhibits coupling to the cavity modes for frequencies near the center of the band gap, thereby reducing the transmission of the grating. Strong field localization at the high energy plasmonic band edge enhances coupling to the cavity modes while field localization at the low energy band edge leads to weak cavity coupling and reduced transmission. [doi:10.1063/1.3638161]

I. INTRODUCTION

Since the first observation in the early 1900s[1,2] of unexpected narrow bright and dark bands in the reflection spectrum of optical gratings, many efforts have been devoted to clarify these anomalous, linear optical phenomena that could not be explained by means of ordinary diffraction-grating theory. The first theoretical interpretation of these effects was provided by Lord Rayleigh,[3] later refined by Fano.[4] Lord Rayleigh predicted the spectral positions of the anomalies resulting from the appearance of new spectral orders. A complete interpretation of Wood's anomalies was reported many years later by Hessel and Oliner,[5] who identified two anomalous manifestations of the grating: (i) the abrupt intensity modulation of diffraction orders at the appearance/fading of new spectral orders, and (ii) resonant-like anomalies. These two effects can occur either separately or simultaneously. The resonant effect matches the excitation of leaky waves supported by the grating for specific spectral orders. The role of surface plasmons in the formation of these anomalies was first discussed after 1968, when Otto,[6] and Kretschmann and Raether[7] reported the excitation of surface plasmons on continuous metal films.

In 1998 Ebbesen *et al*.[8] demonstrated the extraordinary optical transmission (EOT) of light through a metal layer perforated with cylindrical, sub-wavelength holes. The role of surface plasmon polaritons was central in the explanation of the EOT effect. Several authors have reported extraordinary transmission from one-dimensional (1-D) sub-wavelength slits instead of holes from the microwave to the UV range.[9–14] However, narrow slits do not behave like cylindrical apertures. The former is dominated by the transverse electric magnetic (TEM) waveguide mode propagating inside the slits. The latter does not support TEM modes.

[a]Email: ddeceglia@aegistg.com

A 1-D metal grating composed of rectangular slits supports wide-band Fabry-Perot-like resonances[15] whose dispersion can be significantly altered by the presence of the grating. The main effect of the periodicity is the activation of surface modes. Without the grating only an evanescent wave coupling mechanism (i.e. a typical prism coupling) can excite surface modes. The additional wave-vector introduced by the grating along the parallel direction, $k_G = 2\pi/p$, where p is pitch size, induces surface modes on the grating located at frequencies above the light line. It is well-known that excitation of surface modes in the presence of holes/slits can either enhance[16–19] or inhibit[20–26] light transmission. The dispersion of a surface plasmon is[25,27] $k(\omega) = \frac{\omega}{c}\sqrt{\frac{\varepsilon_1\varepsilon_2}{\varepsilon_1+\varepsilon_2}}$, where ε_1 and ε_2 are the permittivities of the adjacent materials. For an air-metal interface (ε_1=1 and complex ε_2) in the terahertz and microwave regimes $k(\omega) \to \frac{\omega}{c}$, while at IR and shorter wavelengths the curve is well detached from the light line in air ($k = \omega/c$), as it bends toward the surface plasmon resonance, $\omega_{sp} = \sqrt{\frac{\omega_p}{1+\varepsilon_2}}$; ω_p is the plasma frequency of the metal. When the metal surface is patterned with a periodic arrangement of grooves or slits, the surface plasmon polariton is itself a resonant part of the diffracted energy:[28] as such it may also be interpreted as a particular case of this mode, and should be studied in relation to all the phenomena involved in the diffraction process. Moreover, the characteristic wavelength of this mode and its effective refractive index dispersion may be altered by the geometric parameters of the grating, i.e. aperture size, film thickness, grating pitch.[29] The dispersion of surface waves may be engineered[30] by properly structuring the surface, even in the presence of perfect metallic screens. For example, for wavelengths close to array periodicity the transmission maxima of one-dimensional (1D) periodic arrays of slits follow the dispersion relation of bound surface waves.[31] These modes become leaky when $\lambda < 2p$, and their dispersion, which is much different from the dispersion of the unperturbed surface plasmon, is governed by the geometrical parameters of the grating and the finite conductivity of the metal.

In what follows we will show that the main effect of the grating is the creation of a band gap for surface plasmons along the grating surface, which induces: (i) transmission suppression through the grating for photon inside the plasmonic band gap; (ii) enhancement and suppression of transmission through the grating at the high and low energy band edges of the above mentioned plasmonic band gap. We will also present a detailed study of the linear optical response of metal gratings for TM polarization, focusing on symmetric, rectangular slits carved on silver layers, as a function of the geometric parameters. In section II we show the dynamical interaction of cavity and surface resonances in going from the single slit case to the infinite array scenario and, in the case of an infinite array, by varying the pitch size. In section III we discuss the origin of the plasmonic band gap and enhanced transmission at the high-energy edge of this forbidden gap. Finally, in section IV we study the transmission properties of the grating as a function of incident angle, aperture size of the slits, and grating thickness. These parameters are varied to emphasize how: (i) the plasmonic band gap follows the dispersion of the unperturbed surface plasmon; (ii) the air filling ratio influences the spectral position of the band gap; (iii) the plasmonic band gap is modified when guided modes are cut off.

II. FROM A SINGLE SLIT TO INFINITE ARRAYS: INFLUENCE OF THE GEOMETRICAL PARAMETERS ON THE TRANSMISSION RESPONSE

We begin by analyzing the problem of a single rectangular slit carved on a silver substrate (see Fig. 1(a)). All calculations and results reported in this paper were obtained using at least three different computational methods that yield nearly identical results: a commercial code based on the Finite Element Method (Comsol Multiphysics);[32] a 2D-FDTD, and a time-domain FFT-BPM whose details have been discussed elsewhere.[33,34] Some slight differences are observable only in proximity of the Wood's anomaly, where the use of long temporal windows is required to capture the very narrow spectral features around these regions. The dispersion profile of silver[35] was fitted using a two-oscillator Lorentz-Drude model to capture free and bound electron contributions to the linear dielectric constant in the visible and near-IR ranges. The influence of the geometric parameters and their respective dependence on the impinging wavelength was considered in an attempt to extract information about the nature of the interaction between the geometrical features and the transmission

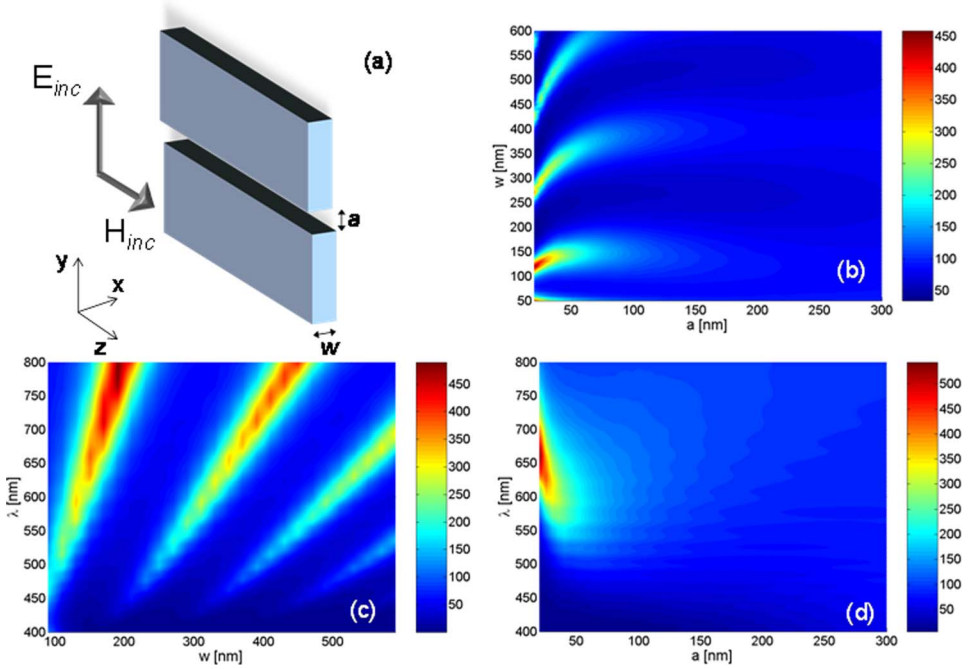

FIG. 1. (a) Sketch of the simulated, single aperture structure and incident polarization; three free parameters have been varied in turn; (b) Two dimensional transmission map for a single slit carved in a silver film for an impinging wavelength $\lambda = 600$nm and variable a and w. (c) transmission coefficient for a variable incident wavelength and varying w; $a = 32$nm; (d) transmission coefficient for a variable impinging wavelength and varying a; $w = 135$nm.

response. As shown in Figs. 1(b)–1(d), a single slit exhibits marked resonant behavior similar to that of Fabry-Perot resonances. Surface modes are poorly coupled to the incident light but the Fabry-Perot waveguide modes couple strongly with the incident light at the resonant wavelengths $\frac{m\lambda_0}{2n_{eff}}$, where m is an integer and n_{eff} is the effective index of the metal-air-metal waveguide. The resonance transmission peaks are governed by the thickness of the metal layer w and slit size a: Fig.1(b) is obtained by considering a plane wave tuned at $\lambda = 600$nm impinging at normal incidence on a single slit with variable size and film thickness (a and w vary in the ranges 20nm-300nm and 50nm-600nm, respectively). Transmittance is normalized to the portion of energy illuminating the slit.

As already pointed out elsewhere,[14,17,36] these kinds of resonances are characterized by significant field localization inside the isolated slit and they induce enhanced transmission without any contributions from surface corrugations or any grating effects. In a single slit, in fact, the transmission process is mostly driven by the TM fundamental mode, whose dispersion is strongly influenced by metal conductivity and slit size. If one considers a waveguide made by two parallel plates separated by a free-space gap, the effective index of the fundamental TM mode is exactly equal to one only in the case of a perfect electric conductor (PEC): in that case the field profile inside the gap region is constant, and zero in the metal. The introduction of a finite conductivity allows the mode to penetrate inside the metal thus increasing the effective index. The dispersion of this modified mode then follows metal dispersion. Moreover, even at microwave wavelengths, where the conductivity is very high, if the sub-wavelength gap is small enough it will show an effective index slightly higher than unity.[13] At optical frequencies light inside the waveguide can penetrate strongly into the metal walls leading to effective indices of order 2 or more, thus providing a strong index contrast at the end-faces of the open cavity.

Another effect that should be considered when the waveguide is abruptly truncated is the strength of the coupling between the guided mode and free space: even when the surrounding metal is assumed to be a PEC the effect of truncation produces a spectral shift of the Fabry-Perot resonances, which should be added to the above mentioned shift induced by the finite conductivity of metal.

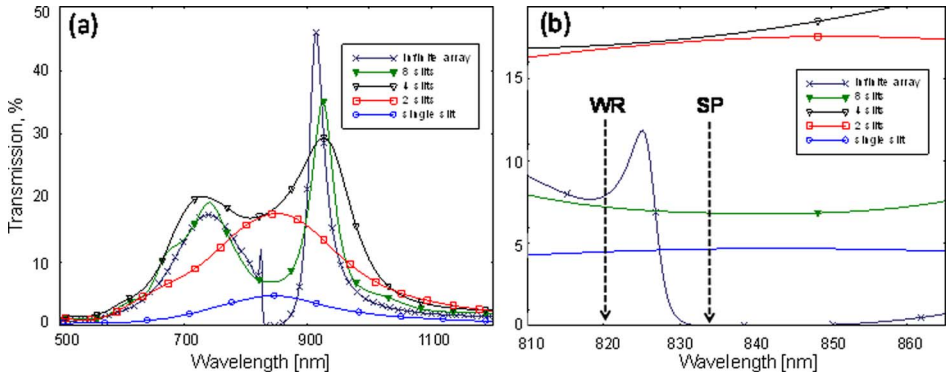

FIG. 2. (a) Comparison of transmission spectra at normal incidence showing the formation of a band gap related to the array periodicity. Using two slits (red curve, square markers) instead of one (blue curve, circle markers) the spectrum shape does not change appreciably and the transmittance more than doubles (red line, square markers). With 4 (black line, empty triangle markers) and 8 slits (green line, full triangle markers) a dip appears near the Wood-Rayleigh minimum position, which is more pronounced for increasing number of slits. In the limit of an infinite array the dip turns into a broad band gap (dark blue line, cross markers). (b) Zoom of (a) in the neighborhood of the transmission minimum. WR is the Wood-Rayleigh condition where the incident wavelength is equal to the pitch ($\lambda = p$), SP is the wavelength at which the unperturbed air-metal surface plasmon matches the grating pitch ($\lambda_{SP} = p$). The real part of the effective index of the unperturbed SP is $\sim$1.02 providing a 14 nm difference between the WR condition and the condition when the SP wavelength equals the grating pitch. The transmission spectra include energy in the zero and first diffraction orders.

The existence of the main propagating mode supported by the parallel-plate waveguide leads to significant enhancement of the transmission that approaches 500% with respect to the energy that impinges on the geometrical area of the isolated slit. Resonant behavior is also evident in Figs.1(c) and 1(d). The figures were obtained by varying only one of the parameters (w in Fig.1(c) and a in Fig.1(d)) and the incident wavelength, tuned in the visible range. The other geometrical parameter was arbitrarily fixed to $a = 32$ nm (Fig.1(c)) and $w = 135$ nm (Fig.1(d)).

A multiple slit geometry structured in a one dimensional periodic array introduces the pitch as an additional degree of freedom. It is well known that adding more slits does not enhance significantly the transmission value itself, which indeed tends to saturate for more than 6 slits.[23,36] However, this argument does not hold under certain circumstances: if pitch size is close to one of the Fabry-Perot-like resonances the spectral response can be significantly altered, as demonstrated in reference (37) for a PEC grating and for metals at microwave or THz frequencies. In what follows we will explore the scenario in which the perforated metal operates at optical frequencies and the dispersion of the smooth air-metal surface plasmon $k(\omega) = \frac{\omega}{c}\sqrt{\frac{\varepsilon_1\varepsilon_2}{\varepsilon_1+\varepsilon_2}}$ is well detached from the light line. As an example, in Fig. 2(a) we show the transmission spectrum at normal incidence for a single slit (blue line-circle markers) compared to the transmission spectra of multiple-slit arrays having increasing number of slits, and to an infinitely long array (dark blue line-cross markers). Aperture size is fixed at $a = 32$nm, film thickness is $w = 200$nm, and pitch size is $p = 820$nm. For the grating having a finite number of slits the transmission is calculated using a beam having 10λ-wide top-hat shape. For the infinite array we simulated an input plane wave and periodic boundary conditions. This kind of arrays is usually fabricated by depositing metal films on substrates such as Si, pyrex or glass using thermionic e-beam evaporation or sputter systems. Thicknesses can be easily controlled in both systems. Once the metal film has been properly deposited the slits are customarily milled by means of a focused ion beam system. For example in Ref. 37 one dimensional patterns of extremely sub-wavelength slits (as small as 32nm with a pitch of 400nm) have been fabricated on a 200nm-thick gold film using a Ga ion beam controlled by a Raith ELPHY Quantum software/hardware system with an accelerating voltage of 30 keV and an ion current of 30 pA. However, it is worth stressing that the presence of a substrate does not significantly alter the physics of the structure, inducing only a spectral shift of Fabry-Perot and plasmonic resonances. For this reason, we study the effect of multiple slits considering the simple case in which the structure is a free-standing grating surrounded by air.

By choosing pitch size equal to the Fabry-Perot-like resonance wavelength we are introducing interference between the Wood's anomaly (onset of the first-order diffracted wave propagating along the grating surface) and the Fabry-Perot cavity resonance of the system. In going from one to two slits the resonance narrows and the maximum transmission increases. With just a few more slits the Wood's anomaly effect becomes evident, so that the Fabry-Perot resonance undergoes strong reshaping driven by the periodicity of the array.

The interference between propagating and evanescent orders diffracted by the grating induces a split of the original resonance with the introduction of a transmission minimum. The effect becomes even more pronounced in the limit of an infinite number of slits (dark blue line, cross markers), for which the dip becomes a wide gap and a sharp transmission edge appears at a slightly blue-shifted wavelength. As also happens with structures that are periodic on the scale of the wavelength of the impinging light, the addition of more periods in the structure favors the opening and widening of a band gap, whose center and width are controlled mainly by the number of periods in the structure. A careful look at the position of the transmission minimum (Fig.2(b)) highlights the difference between the perfect conductor case, where the minimum occurs at the Wood-Rayleigh wavelength (indicated in Fig.2 by the WR arrow),[38] and the finite-conductivity metal case, where the transmission shows a deep minimum where the air-metal surface plasmon wavelength matches grating pitch (indicated in Fig.2 with the SP arrow). While in this case the shift between the WR and SP points is 14nm, it increases at higher frequencies, where the surface plasmon effective index is larger, as we will show in the next example.

The presence of band gaps in the surface plasmon dispersion curve was observed by Ritchie *et al*. on Al and Au shallow gratings.[39] Moreover, the similarity of a surface plasmon traveling on a corrugated surface and a photonic band gap structure, as well as the relationship between the band gap and the periodicity, have already been discussed for shallow and deep grooves on metal films.[40,41] Nevertheless, this structure has an additional feature with respect to those described in (Refs. 39–41): the slits traverse the entire thickness of the metal layer, so that the resulting Fabry-Perot resonances excited inside the slits are potentially able to couple surface waves from the input to the output section of the grating. When dealing with an infinite array of slits there are three other mechanisms absent in the single slit case: (1) the interaction between diffracted waves; (2) the introduction of surface waves triggered by the reciprocal lattice vector of the grating; (3) the strong perturbation induced by the grating itself on surface waves.

From now on we will focus only on infinite arrays. These structures fully preserve the Fabry-Perot resonance positions, the characteristics of their single-slit's counterpart, and remain dominant features. However, by varying pitch size p one can either isolate these Fabry-Perot modes, or cause them to interact with the diffraction process taking place on the grating. In Fig.3(a) we plot the transmission of a single, rectangular slit with an aperture size $a = 32$nm and a length $w = 300$nm that pierces the silver layer from side to side. In this spectrum two resonances can be easily recognized around 550nm and 1100nm. If one considers an array of these slits with pitch size $p = 280$ nm, the resulting structure is in the zero-order grating condition:

$$\frac{p}{\lambda} = \frac{1}{n_{in}\sin\theta + \max\left(n_{in}, n_{out}\right)}, \tag{1}$$

where θ is the incident angle and n_{in} and n_{out} are the input and output refractive indexes, respectively. As a result, the grating is sub-wavelength and the only forward-propagating diffracted wave is the zero-th order. All higher orders are evanescent. As displayed in Fig.3(b), there are no significant modifications in the shape of the spectrum, which matches quite well the resonances of an isolated cavity of the same size. The reason for this derives from the simple observation of the position of the Wood's anomaly wavelengths, $\lambda_W = |\frac{\sin\theta}{\lambda_{0,inc}} + \frac{m}{p}|^{-1}$, where $m = \pm1, \pm2, ...$, θ is the angle of incidence and $\lambda_{0,inc}$ is the incident wavelength. We emphasize that the Fabry-Perot cavity modes of the single slit, named H1 and H2 in Fig. 3(a), guarantee a total transmission of 80% and 50% (Fig.3(b)), respectively, even with a metal film 300nm-thick, which in this operating regime is virtually opaque without apertures. On the other hand, by tuning the period of the grating inside the resonance bandwidth one is able to alter at will the transmittance function, and to reshape one or more Fabry-Perot resonances simultaneously.

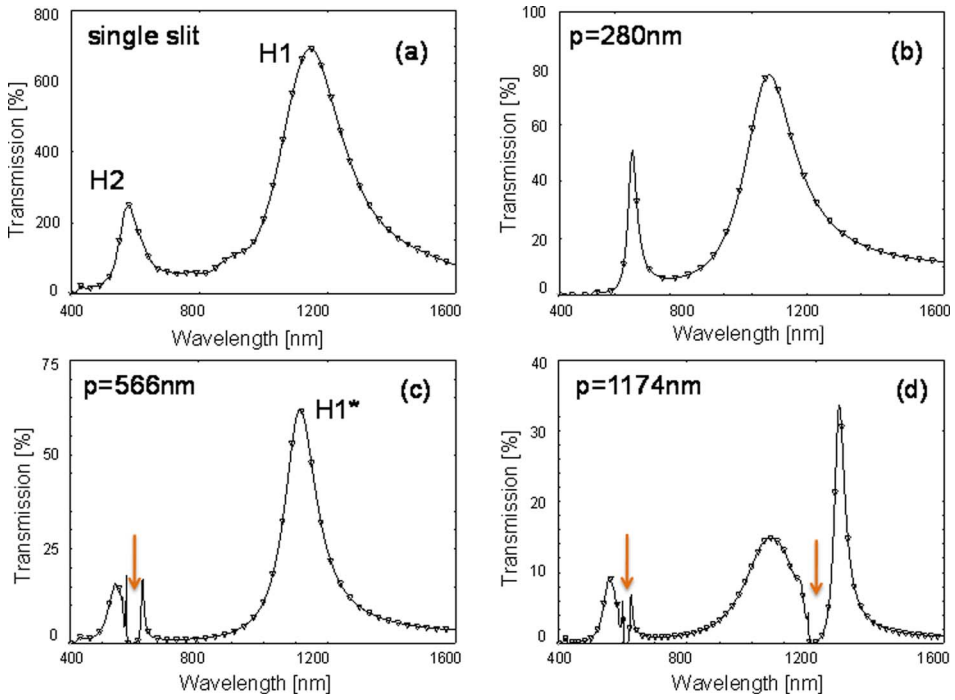

FIG. 3. (a) Transmission spectrum of a single 32 nm slit in a 300 nm silver film, *normalized with respect to the energy incident on the geometrical area of the aperture*. The transmission spectra at normal incidence for infinite silver gratings with different pitch sizes are reported in (b), (c) and (d), *normalized with respect to total incident energy*. The geometrical parameters for the gratings are $a = 32$ nm, $w = 300$ nm and (b) $p = 280$ nm, (c) $p = 566$ nm, (d) $p = 1174$ nm. Figures (b), (c) and (d) show the formation of 0 (b), 1 (c) and 2 (d) band gaps in the spectra, caused by the periodicity of the array. Figs. c and d include energy transmitted into the zero and first order.

As Figs. 3(c) and 3(d) show, a periodicity $p = 566$ nm or $p = 1174$ nm splits the horizontal resonances and creates one band gap (Fig. 3(c)) and two band gaps (Fig. 3(d)) respectively. The effect of this interaction manifests itself with the near-complete inhibition of transmission. This condition takes place for those surface plasmon wavelengths that match *exactly* the grating pitch, so that at normal incidence $\lambda_{sp} = p/m$. The impinging light then exploits the sub-wavelength features of the grating to find the missing momentum that allows the potential propagation of a surface plasmon without resorting to any other evanescent coupling mechanisms. The use of the term 'potential' is not fortuitous since, at the transmission minimum wavelength, the grating is simultaneously coupling the incident plane wave onto the surface plasmon mode while de-coupling it in the backward direction. This mechanism may be also explained using another point of view: after the grating delivers the incoming energy to the surface plasmon wave (first-order diffraction mode) this guided mode encounters an effective plasmonic band gap along the air- metal interface induced by the alternation of air sections (the thin slits) and metallic sections, that prevents any surface mode from propagation over a certain bandwidth.

The spectrum of Fig. 3(c) is magnified and shown in Fig. 4(a) around the wavelength $\lambda_0 = n_{spp}p$, with $n_{spp} = \mathrm{Re}\{\sqrt{\frac{\varepsilon_{Ag}}{\varepsilon_{Ag}+1}}\}$.[25]

One may recognize a sharp resonance at $\lambda_v = 573$ nm (denoted by V resonance in the figure), a gap located in the neighborhood of the unperturbed plasmonic wavelength, and two wider maxima on each side of these anomalous spectral features (the V state and the gap introduced by the periodicity), which are reminiscent of the Fabry-Perot resonance. We name H2* the hybridization of the Fabry-Perot resonance H2 (excited by the single–slit) with the surface resonant phenomenon triggered by the diffraction grating. While the coupling between cavity and surface modes has been indicated as the mechanism responsible for EOT,[42,43] we stress the role of this hybridization also in the formation of the plasmonic band gap.

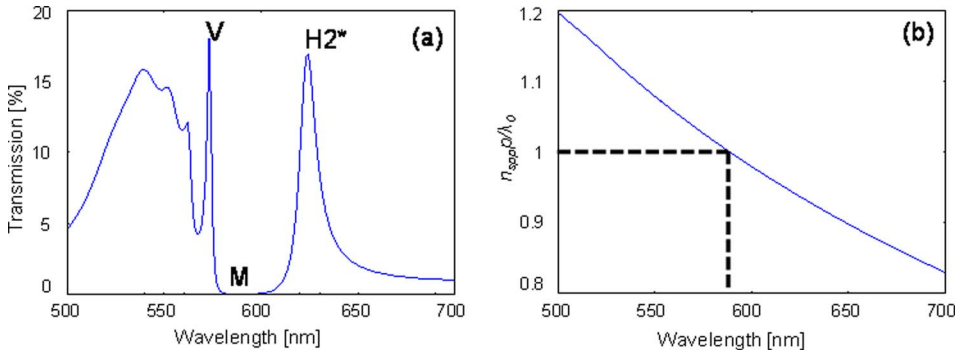

FIG. 4. (a) Transmission spectrum at normal incidence of an array of sub-wavelength slits with the following geometrical parameters: $a = 32$ nm, $w = 300$ nm, $p = 566$ nm; (b) Surface plasmon polariton wavelength in normalized units plotted as a function of the incident wavelength. The highlighted point represents the condition for the band gap in the surface plasmon polariton dispersion relation, which leads to a formation of the transmission minimum M at 588 nm shown in Fig. 4 (a). The WR condition at 566 nm is separated 20 nm from point M.

The last point marked in Fig.4(a) is the minimum M, which is strictly related to the formation of a forbidden plasmonic band gap. The location of M ($\lambda_M = 588$nm) is explained in Fig. 4(b), where we provide a graphical solution of the equation $\lambda_0 = n_{\mathrm{spp}}p$ for the grating under consideration. A more detailed discussion on the field localization across the band gap region will be given in the next section.

III. PROPERTIES OF THE PLASMONIC BAND GAP AND BAND EDGES

The most common photonic band gap structure is perhaps a dielectric mirror composed of multilayer dielectrics with quarter-wave layers. The spectral width of the gap depends on the index contrast between the two dielectrics, while the depth of the gap depends on the number of periods. At the band edges transmission is unity, group velocity reaches a minimum and there is strong field localization. At the high energy band edge the electric field localizes in the low index layers and at the low energy band edge the electric field localizes in the high index layers. Field localization effects at the photonic band edges have been observed in the spontaneous emission spectra of GaAs/AlGaAs multilayer light emitting diodes: emission from the GaAs layers is enhanced and suppressed at the low and high energy band edges respectively.[44] If one of the dielectrics composing the multilayer structure is lossy, the low group velocity and field localization cause an asymmetry in the transmission and absorption at the band edges but the reflection is only weakly affected by the loss.

We calculated transmission (T), reflection (R) and absorption (A) for a 50-periods, 1D multilayer stack obtained alternating 32nm-thick layers having a refractive index equal to 1.0 (air) with 534nm-thick-layers with an index n_{spp} equal to the real part of the effective refractive index of the surface plasmon propagating on a smooth air/silver interface (Fig. 5(a)). This structure has a periodicity p=566nm equal to the pitch of the grating described in Fig. 4(a) and it shows the formation of a band gap centered at 588nm (solid blue and red lines in Fig. 5(b)). By introducing losses in the 32nm thick layers (whose refractive index is now 1.0+i0.02) we observe an asymmetric response in the transmission and absorption spectra (dotted blue and black lines in Fig. 5(b), respectively), similar to the one described above for the quarter wave stack with losses. The inclusion of losses in the air layers mimics the coupling of energy into the guided modes of the slits. These modes can be excited either by energy coming from the surface, i.e. surface plasmons, or by energy coming from the free-space (see Fig.1(a)). Reflection is almost identical for the multilayer stack with and without losses (Fig. 5(b), solid and dotted red lines). Worthy of note is the fact that due to field localization at the band edges absorption losses at the high energy band edge are much larger than at the low energy band edge (black dotted line).

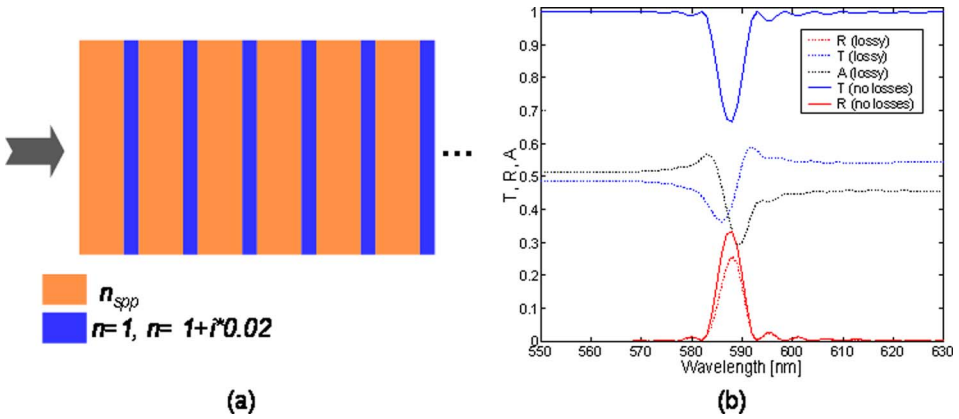

FIG. 5. (a) Sketch of a 50-periods 1D multilayer stack obtained alternating 32nm thick air layers with a 534 nm thick material having the same refractive index of the unperturbed surface plasmon propagating at a silver/air interface. We analyze this structure with and without losses in the low-index, air layers; (b) transmittance (blue lines), reflectance (red lines), and absorption (black line) for the structure (a). The figure illustrates the effects of adding losses to the 32 nm thick layers: solid lines refer to the multilayer without losses in the 32-nm layers (n=1), while dotted lines refer to the structure with losses in the 32nm-layers (n=1.0+i0.02).

Let us now move back to the metal grating described above (a=32 nm, p=566 nm, and w= 300 nm, transmission spectrum plotted in Fig 4(a)). We studied the transmission properties of the structure by launching a surface wave in the transverse direction (see Fig. 6(a)). Fig 6(b) shows the transmission spectrum of the structure in Fig.6(b): one can easily see that the basic features of the plasmonic band structure experienced for the metal grating studied in the configuration of Fig.4(a) appear in the same wavelength range. In particular a zero transmission state centered at 588 nm is a clear indication of the formation of a plasmonic band gap (surface plasmon wavelength is equal to the period of the grating.)

Other analogies between the metal grating and a 1D periodic structure across the band gap region may also be found by analyzing field localization. The magnetic field distribution depicted in Fig. 7(a) and 7(c) corresponds to typical first and second order FP resonances, respectively. Fig 7(a) refers to the point H1* of Fig. 3(c), where the only diffracted wave is the zero-order and the grating is far from the conditions necessary to excite any significant surface activity. The lack of surface waves is confirmed by the absence of strong magnetic fields at the input and output interfaces and by the absence of any significant perturbation of the Poynting vector (yellow arrows in Figs. 7), even in the near-field of the aperture. In Fig. 7(c), which corresponds to H2* of Fig 4(a), there is some evidence of surface activity due to the proximity of the plasmonic band gap, but the FP resonance is the dominant feature. One may conclude that from a diffraction point of view the slits do not interact, cannot see each other, and act almost undisturbed in the formation of the transmission resonance found for the single-slit.

In contrast, abrupt changes of the field localization are evident when surface plasmons interact with FP resonances. These variations can be linked in straightforward fashion to the strong perturbations of the diffraction efficiencies expected around the Wood's anomalies. We observe that an enhanced reflection state from the grating, the point M in Fig. 4(a), is very close to an enhanced transmission state, the point V on the same figure, and that the light suppression effect has a non-negligible bandwidth of several tens of nanometers. Based on the plasmonic band gap features depicted in Fig. 7(b), the point M, which is the wavelength of minimum transmission through the grating, corresponds to the center of the plasmonic band gap. Point V (Fig. 7(d)), where the transmission through the grating is large, corresponds to the plasmonic band edge. Inside the plasmonic band gap the propagation of surface modes is forbidden, and at the band edge propagation is allowed and accompanied by low group velocities and strong field localization. It is clear from the magnetic field localization that a hybrid mode embracing the whole grating (the sub-wavelength slits and the metal-air interfaces) is resonating collectively, allowing the transfer of light to the other side of the

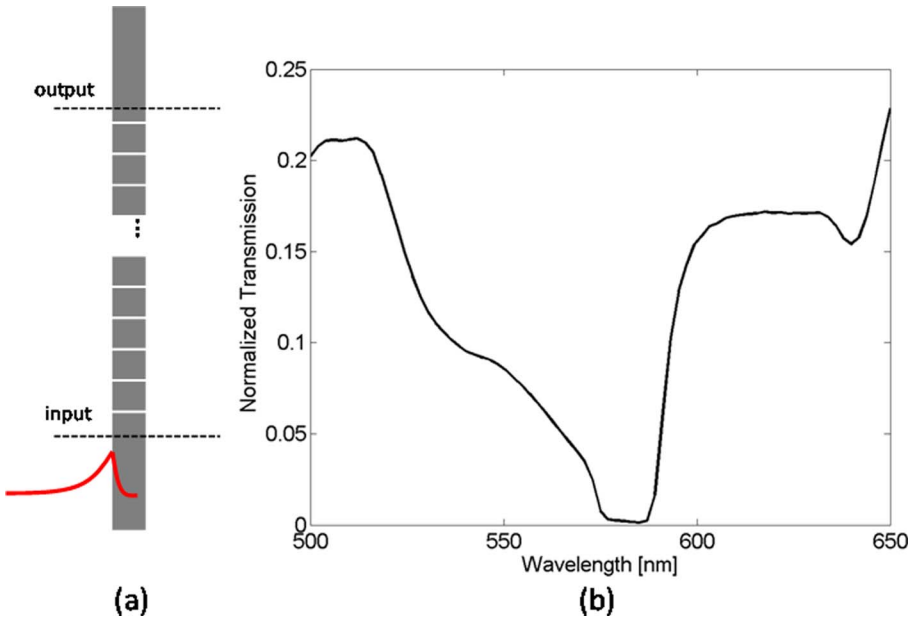

FIG. 6. (a) Sketch of the structure analyzed in the transverse direction. The SP is launched from the lower-left side at the input section and transmission is calculated by integrating the Poynting vector on the upper-left side of output section. The grating geometry is the one described in Fig. 4 (a=32 nm, w=300 nm, p=566 nm) and number of periods is 60. (b) SP transmission spectrum. The transmission has been normalized to the transmission of the SP across a smooth silver surface of the same length (about 35μm). Based on the spectrum, the plasmonic band gap is ~20 nm wide and centered near the condition for the SP wavelength equal to the period of the grating.

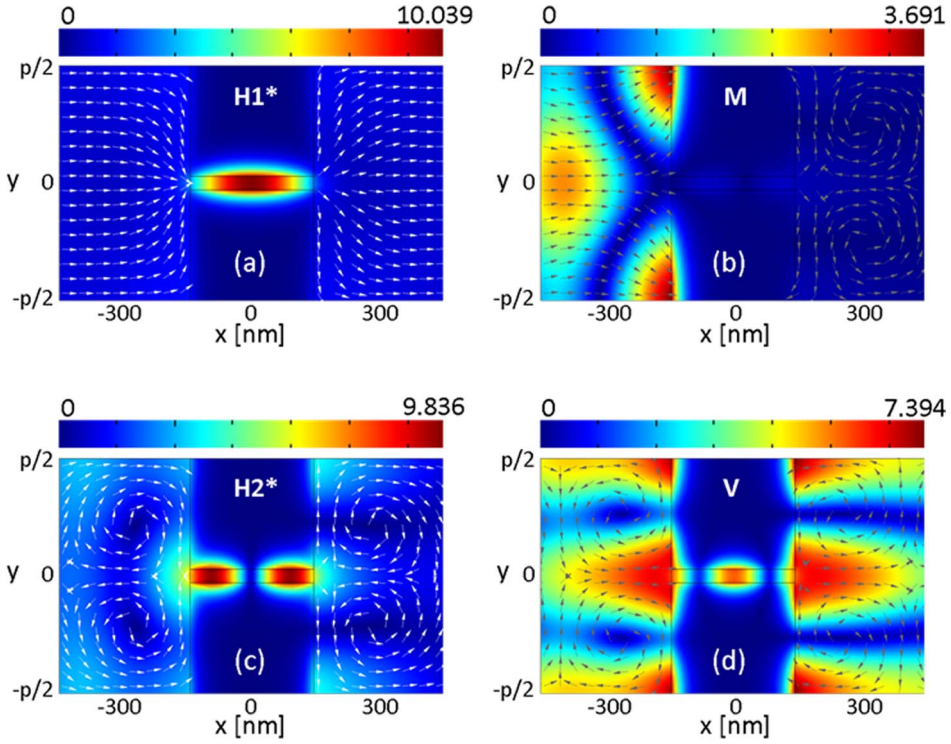

FIG. 7. (a) The color scale is the magnetic field amplitude at $\lambda = 1.115$ μm (point H1* in Fig. 3(c)) for an array with the same parameters described in Fig. 3(c) and Fig. 4(a) with a=32 nm, w=300 nm, and p=566 nm. The arrows sketch the normalized Poynting vector distribution; (b) Same as (a) at $\lambda = 0.588$ μm (point M in Fig. 4(a)); (c) Same as (a) at $\lambda = 0.630$ μm (point H2* in Fig. 4(a)); (d) Same as (a) at $\lambda = 0.573$ μm (point V in Fig. 4(a)).

grating. In fact, the reader should observe that coupling between surface waves excited on each side of the grating can be achieved only through the slits, given that the silver layer is much too thick (300nm) to allow coupling through its bulk sections. At the low energy plasmonic band edge transmission is prohibited but it is not due to the inhibition of surface modes. Rather, it is due to a π phase shift in the field localization that occurs in going from one band edge to the other. The interaction of surface plasmons with the grating leads to the formation of a plasmonic band gap with suppressed transmission inside the gap and at one band edge, and enhanced transmission at the other band edge.

As already demonstrated for light transmission through single apertures surrounded by periodic grooves,[45–47] leaky plasmons improve light coupling on the input interface and provide enhanced transmission and high broadside directivity at the exit interface of the grating. The same mechanism mediates the formation of the modes V and H2*. At the minimum point M, the incident light bends in front of the aperture and deflects back as if the grating were a smooth surface. The grating then acts as a perfect mirror, allowing the excitation of the unperturbed surface plasmon polariton with a minimum located in front of the slit. This causes a subsequent re-irradiation of light on the input side of the grating: this virtually *chokes* the slits with a surface resonant state. Later we will show how this effect persists regardless of slit thickness and impinging wavelength, as long as the condition $\lambda_{sp} = p$ is satisfied. Absorption of ∼2% and reflection of ∼98% at point M are consistent with values one expects from a smooth, free-standing silver interface. On the other hand, absorption maxima occur at both the V and H2* states. In particular, Joule heating is well confined within the slit for the H2* FP resonance, while it involves both the slits and the input and output interfaces at the V state.

IV. SURFACE PLASMON COUPLING AND RAYLEIGH MINIMUM CONDITION: HOW ARE THEY LINKED?

A. Angular analysis

In the previous section we showed how the formation of the band gap is directly linked to the periodicity of the structure and how the fields localize across the forbidden region. We also demonstrated how to manage the interaction of surface waves alongside cavity resonances (Figs. 3) by appropriately tuning the array periodicity. Another effective way to control the interaction is to tilt the structure and to scan the transmission at different incident angles. Unlike all the results reported so far, the transmission response in Fig. 8 is obtained by varying the wavelength and the angle of the incident plane wave. The parameters of the array of Fig.8 are the same as those of Figs. 4. We stress that the normal incidence transmission plotted in Fig. 4(a) is sketched along the $k_{//}$=0 axis (for angular frequencies between $2.69 \cdot 10^{15}$ rad/s and $3.77 \cdot 10^{15}$ rad/s), and forms a band gap around the zero transmission state at $\lambda = 588$nm ($\omega = 3.18 \times 10^{15}$ rad/s).

At least two more observations may be inferred by looking at Fig. 8: i) by tilting the incident angle the plasmonic band gap can cross the cavity mode orders of the system and locate the zero transmission state at different wavelengths within the Fabry-Perot cavity modes (FP1 or FP2 in Fig. 8), which are almost invariant with the incident angle; ii) the conditions for the potential excitation of the unperturbed (smooth, metal-air interface) surface plasmon, $k_{sp} = \left|k_0 \sin\theta + m^{2\pi}/p\right|$, denoted by the white curves on the map, coincide systematically with the formation of a transmission minimum equal to the point M described in Fig. 4(a) and Fig. 7(b). However, the position of the band gap created in the spectrum is not invariant with aperture size, and helps to distinguish the roles of the Wood's anomaly and the SP.

B. Aperture-size analysis

In Fig. 9(a) we report the transmission map on a logarithmic scale, obtained by varying incident wavelength and aperture size, fixing film thickness to 300nm-thick and pitch size p=566nm. The incident wavelength is varied near the characteristic wavelength that excites a surface plasmon at an effective wavelength equal to pitch size. Aperture size, or air filling ratio, is varied from 20nm (air filling ratio ∼3%) to 560nm (air filling ratio ∼99%). Transmission approaches 100% by increasing

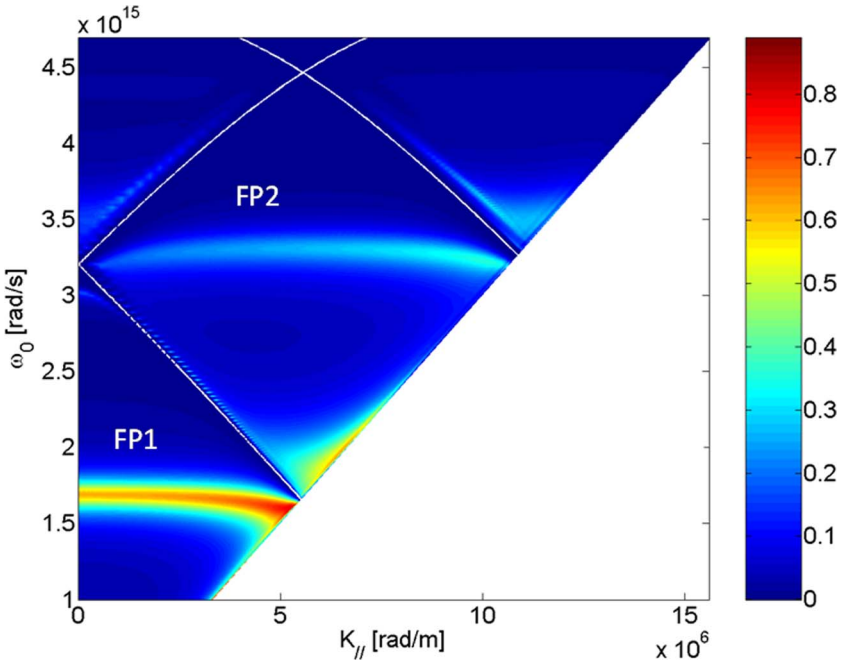

FIG. 8. Transmission spectrum as a function of the in-plane wave vector and angular frequency for an array of slits having the following geometrical parameters: $a = 32$nm, $w = 300$nm, p=566nm. The white lines refer to the folded dispersion curve of the surface plasmon.

the air filling ratio, since we are reducing the amount of metal in the structure. The most interesting feature of this map is the section highlighted by the dashed yellow and white lines, both marked with the label M in Fig. 9(a). These lines correspond to the minimum transmission state described above, occurring at $\lambda_{sp} = p$. According to the results presented in the previous sections, the zero transmission state falls systematically at the wavelength where the grating wave vector $2\pi/p$ excites the unperturbed surface plasmon.

As the air filling ratio increases and the structure becomes less metallic, three effects take place: (i) the effective refractive index of the fundamental TM mode in the slit waveguide decreases and tends to unity (all the Fabry-Perot resonances shift toward shorter wavelengths); (ii) the bandwidths of the Fabry-Perot resonances are broader; (iii) the condition for the minimum transmission state moves from the surface plasmon band gap (dashed yellow line in Fig. 9(a) to the classic Rayleigh minimum condition (dashed white line in Fig. 9(a)), occurring at $\lambda = $ p. Following the minimum spectral position, the transition from the plasmonic minimum (dashed yellow line) to the purely photonic minimum (dashed white line) is evident by looking at the slope of the white line, starting from an air filling ratio of $\sim$25%. In other words, the condition for the coupling and simultaneous back-radiation due to the surface plasmon band gap at the input interface is preserved as long as the apertures are small enough ($a < 140$nm for this particular grating). Under these circumstances the magnetic field always exhibits a minimum at the center of the aperture (see Fig. 7(b)).

C. Thickness analysis

We also calculated the transmission response as a function of both impinging wavelength and film thickness. Both aperture and pitch are constant and equal to $a = 32$nm and $p = 566$nm, respectively. In Fig.10 one may easily recognize some of the features of Fig.1(c), which was obtained for a single aperture of the same size: the first and the second order Fabry-Perot modes occur at the same spectral positions and are altered only where they are crossed by the transverse resonating surface modes (horizontal section $\lambda_{sp} = p$ highlighted in white).

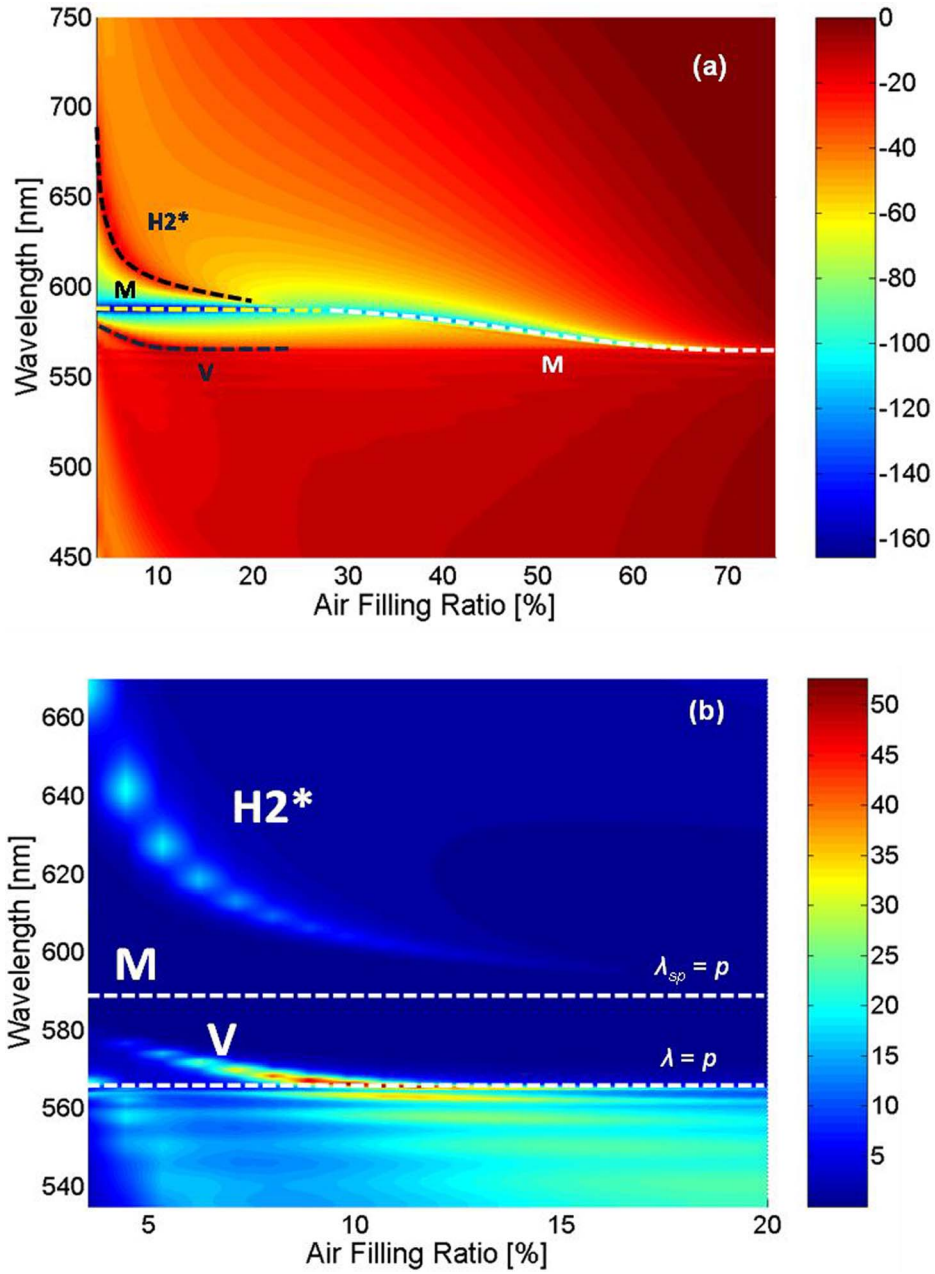

FIG. 9. (a) Transmission map on a logarithmic scale (decibels) at normal incidence for a silver grating whose thickness is $w = 300$ nm and pitch $p = 566$nm. (b) Magnification of (a) plotted on a linear scale (color scale in percentage of the total incident power) to highlight the bending of the transmission maxima H2* and V. The dashed lines indicate the condition $\lambda_{sp} = p$ (labeled M) and the classic Wood-Rayleigh minimum condition $\lambda = p$.

Moreover, two regimes are distinguishable in this map, separated by the vertical dashed line. The region on the right denotes the thick film regime and is characterized by surface waves and FP resonances that interact via the guided modes of the slits. In contrast, in the left region, i.e. thin films, the guided modes of the slits cannot resonate and the enhanced transmission is achieved only through evanescent wave coupling that takes place either inside the slits or through the bulk metal. In particular in this regime the coupling of the input and output surface plasmons induces the formation of long and short range plasmons whose dispersion can be significantly distorted.[48]

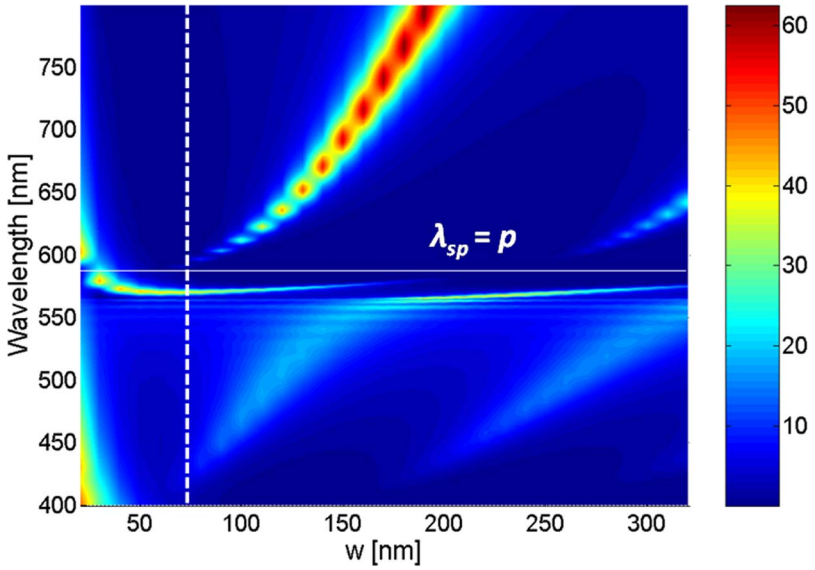

FIG. 10. Transmission map at normal incidence for a silver grating with variable thickness (x-axis), pitch size $p = 566$nm and aperture size $a = 32$nm. The vertical dashed line traces an approximate transition from the thin to the thick film regime. In the thin film region Fabry-Perot-like resonances are cut-off. The horizontal line corresponds to the condition $\lambda_{sp} = p$.

V. CONCLUSIONS

In summary, we have analyzed several fundamental properties of enhanced transmission in metal gratings, showing that it is possible to achieve full control of transmission efficiency. The combined study of a single slit system and its periodic counterpart reveals virtually identical spectral features, except at wavelengths that nearly match the grating pitch. In particular the effect of the interaction of Fabry-Perot modes and surface modes is the opening of a plasmonic band gap, where the simultaneous coupling and back-reflection at the surface plasmon band gap prevent light from coupling into the cavity mode inside the slit. For incident wave-vectors and grating pitches expected to exactly match and excite a surface plasmon, absorption is comparable to the bulk metal case of $\sim$2% and transmission is suppressed by several orders of magnitude.

For gratings with an air filling factor $<$30%, we find that light flow through the slits is inhibited at the wavelength of the surface plasmon band gap. For fill factors $>$30% light flow tends to be inhibited at the classic Wood-Rayleigh minimum condition. On the other hand, leaky surface plasmon waves excited by the grating act like vertical resonating modes that collect the impinging light and interact with Fabry-Perot modes to form hybrid modes and trigger high transmission states at the plasmonic band edge. The hybrid nature of these modes is confirmed by observing field localization properties, and by mapping the behavior of the structure as a function of the air filling ratio, revealing their strong dependence on aperture size. The opening of a plasmonic band gap for surface waves in analogy of photonic band gaps for propagating waves could have important implications particularly in the nonlinear regime, where band edge effects have been shown to exhibit enhanced nonlinear response. The plasmonic band gap may be engineered for a specific application, for example, in harmonic generation, sensing, and surface enhanced Raman scattering (SERS) to name a few.

AKNOWLEDGMENTS

The authors want to thank G. D'Aguanno, N. Mattiucci and M. C. Buncick for stimulating discussions.

[1] R. W. Wood, "On the remarkable case of uneven distribution of a light in a diffractive grating spectrum", Philos. Mag. **4**, 396 (1902).

[2] R. W. Wood, "Diffraction gratings with controlled groove form and abnormal distribution of intensity", Philos. Mag. **23**, 310 (1912).
[3] Lord Rayleigh, "On the Dynamical Theory of Gratings", Proc. R. Soc. London, Ser. A **79**, 399 (1907).
[4] U. Fano, "The theory of anomalous diffraction gratings and of quasi-stationary waves on metallic surfaces (Sommerfeld's waves)", J. Opt. Soc. Am. **31**, 213 (1941).
[5] A. Hessel and A. A. Oliner, "A New Theory of Wood's Anomalies on Optical Gratings", Applied Optics **4**, 1275 (1965).
[6] A. Otto, "Excitation of nonradiative surface plasma waves in silver by the method of frustrated total reflection", Z. Phys. **216**, 398 (1968).
[7] E. Kretschmann and H. Raether, "Radiative decay of nonradiative surface plasmons excited by light", Z. Naturforsch., Teil. A **23**, 2135 (1968).
[8] T. W. Ebessen, H. J. Lezec, H. F. Ghaemi, T. Thio and P. A. Wolff, "Extraordinary optical transmission through subwavelength hole arrays", Nature **391**, 667 (1998).
[9] R. Gordon, "Light in a subwavelength slit in metal: propagation and reflection", Phys. Rev. B **73**, 153405 (2006).
[10] J. Bravo-Abad, L. Martin-Moreno and F. J. Garcia-Vidal, "Transmission properties of a single metallic slit: from the subwavelength regime to the geometrical optical limit, Phys. Rev. E **69**, 026601 (2004).
[11] Y. Xie, A. R. Zakharian, J. V. Moloney and M. Mansuripur, "Transmission of light through slit apertures in metallic films", Opt. Express **12**, 6106 (2004).
[12] F. Yang and J. R. Sambles, "Resonant transmission of microwaves through a narrow metallic slit", Phys. Rev. Lett. **89**, 063901 (2002).
[13] J. R. Suckling, A. P. Hibbins, M. J. Lockyear, T. W. Preist, J. R. Sambles and C. R. Lawrence, "Finite conductance governs the resonance transmission of thin metal slits at microwave frequencies", Phys. Rev. Lett. **92**, 147401 (2004).
[14] M. A. Vincenti, D. de Ceglia, M. Buncick, N. Akozbek, M. J. Bloemer, and M. Scalora, Extraordinary transmission in the ultraviolet range from subwavelength slits on semiconductors, Journal of Applied Physics **107**, 053101 (2010).
[15] J. T. Shen, P. B. Catrysse and S. Fan, "Mechanism for Designing Metallic Metamaterials with a High Index of Refraction", Phys. Rev. Lett. **94**, 197401 (2005).
[16] T. Thio, H. F. Ghaemi, H. J. Lezec, P. A. Wolf, T. W. Ebessen, "Surface-plasmon-enhanced transmission through hole arrays in Cr films", J. Opt, Soc. Am. B **16**, 1743 (1999).
[17] J. A. Porto, F. J. Garcia-Vidal, and J. B. Pendry, "Transmission resonances on metallic gratings with very narrow slits", Phys. Rev. Lett. **83**, 2845 (1999).
[18] L. Martin-Moreno, F. J. Garcia-Vidal, H. J. Lezec, K. M. Pellerin, T. Thio, J. B. Pendry, and T. W. Ebbesen, "Theory of Extraordinary Optical Transmission through Subwavelength Hole Arrays," Phys. Rev. Lett. **86**, 1114 (2001).
[19] F. J. Garcia-Vidal and L. Martin-Moreno, "Transmission and focusing of light in one-dimensional periodically nanostructured metals", Phys. Rev. B **66**, 155412 (2002).
[20] Q. Cao and Ph. Lalanne, "Negative Role of surface plasmons in the transmission of metallic gratings with very narrow slits," Phys. Rev. Lett. **88**, 057403 (2002).
[21] P. Lalanne, C. Sauvan, J. P. Hugonin, J. C. Rodier, and P. Chavel, "Perturbative approach for surface plasmon effects on flat interfaces periodically corrugated by subwavelength apertures", Phys. Rev. B **68**, 125404 (2003).
[22] Y. Xie, A. R. Zakharian, J. V. Moloney, and M. Mansuripur, "Transmission of light through a periodic array of slits in a thick metallic film", Opt. Express **13**, 4485 (2005).
[23] D. Pacifici, H. J. Lezec, H. A. Atwater, J. Weiner, "Quantitative determination of optical transmission through subwavelength slit arrays in Ag films: Role of surface wave interference and local coupling between adjacent slits", Phys. Rev. B **77**, 115411 (2008).
[24] W. L. Barnes, W. A. Murray, J. Ditinger, E. Devaux and T. W. Ebessen, "Surface plasmon polaritons and their role in the enhanced transmission of light through periodic arrays of sub-wavelength holes in a metal film", Phys. Rev. Lett. **92**, 107401 (2004).
[25] H. Raether, *Surface Polaritons on Smooth and Rough Surfaces and on Gratings*, Springer-Verlag, Berlin (1988).
[26] H. Lezec and T. Thio, "Diffracted evanescent wave model for enhanced and suppressed optical transmission through subwavelength hole arrays", Opt. Express **12**, 3629 (2004).
[27] S. Meier, *Plasmonics: Fundamentals and applications*, Springer – New York (2007).
[28] M. M. J. Treacy, "Dynamical diffraction explanation of the anomalous transmission of light through metal gratings", Phys. Rev. B **66**, 195105 (2002).
[29] K. G. Lee and Q-Han Park, "Coupling of Surface Plasmon Polaritons and Light in Metallic Nanoslits", Phys. Rev. B **95**, 103902 (2005).
[30] J. B. Pendry, L. Martin-Moreno, F. J. Garcia-Vidal, "Mimicking surface plasmons with structured surfaces", Science **305**,847 (2004).
[31] J. Garcia-Vidal, L. Martin-Moreno, T. W. Ebbesen, and L. Kuipers, "Light passing through subwavelength apertures", Rev. of Mod. Phys. **82**, 729 (2010).
[32] *Comsol Multiphysics 3.5a*; http://www.comsol.com
[33] R. W. Ziolkowski, "Pulsed and CW Gaussian beam interactions with double negative metamaterials slab", Opt. Express **11**, 662 (2003).
[34] M. Scalora, G. D'Aguanno, N. Mattiucci, M. J. Bloemer, J. W. Haus, A. M. Zheltikov, "Negative refraction of ultrashort electromagnetic pulses", Appl. Phys. B **81**, 393 (2005).
[35] E. D. Palik, *Handbook of Optical Constants of Solids*, Vol. **I**, pp. 353–357, Academic Press - New York (1985).
[36] M. A. Vincenti, M. De Sario, V. Petruzzelli, A. D'Orazio, F. Prudenzano, D. de Ceglia, N. Akozbek., M. J. Bloemer, P. Ashley, M. Scalora, "Enhanced transmission and second harmonic generation from subwavelength slits on metal substrates", Proceedings of SPIE **6987**, 69870O (2008).

[37] M. C. Buncick, P. R. Ashley, M. Scalora, N. Akozbek, M. A. Vincenti, M. Centini, J. D. Fowlkes, I. N. Ivanov, "Investigation on the interaction of Surface Plasmons (SP) with an Electro Optiic Polymer and Development of SP Optical Devices", IEEE Proceedings of 17th Biennal University/Government Industry Micro/Nano Symposium, 128 (2008).
[38] A. I. Fernandez-Dominguez, F. J. García-Vidal, L. Martín-Moreno, "Resonant transmission of light through finite arrays of slits", Phys. Rev. B **76**, 235430 (2007).
[39] R. H. Ritchie, E. T. Arakawa, J. J. Cowan, R. N. Hamm, "Surface-plasmon resonance effect in grating diffraction", Phys. Rev. Lett. **21**, 1530 (1968).
[40] W. L. Barnes, T. W. Preist, S. C. Kitson, J. R. Sambles, N. P. K. Cotter, and D. J. Nash, "Photonic gaps in the dispersion of surface plasmon on gratings", Phys. Rev. B **51**, 11164 (1995).
[41] S. S. Senlick, A. Kocabas, and A. Aydinli, "Grating based plasmonic band gap cavities", Opt. Express **17**, 15541 (2009).
[42] F. Marquier, J. Greffet, S. Collin, F. Pardo, and J. Pelouard, "Resonant transmission through a metallic film due to coupled modes, Opt. Express **13**, 70 (2005).
[43] P. B. Catrysse, G. Veronis, H. Shin, J. T. Shen, and S. Fan, "Guided modes supported by plasmonic films with a periodic arrangement of subwavelength slits", Appl. Phys. Lett. **88**, 031101 (2006).
[44] M. D. Tocci, M. Scalora, M. J. Bloemer, J. P. Dowling, and C. M. Bowden, "Measurement of spontaneous-emission enhancement near the one-dimensional photonic band edge of semiconductor heterostructures," Phys. Rev. A **53**, 2799 (1996).
[45] A. A. Oliner, D. R. Jackson, "Leaky surface-plasmon theory for dramatically enhanced transmission through a sub-wavelength aperture, Part I: Basic features", Proceedings of IEEE Antennas and Propagation Society Symposium, Columbus, OH, **2**, 1091 (2003).
[46] D. R. Jackson, T. Zhao, J. T. Williams, A. A. Oliner, "Leaky surface-plasmon theory for dramatically enhanced transmission through a sub-wavelength aperture, Part II: Leaky-Wave Antenna Model", Proceedings of IEEE Antennas and Propagation Society Symposium, Columbus, OH, **2**, 1095 (2003).
[47] D. R. Jackson, J. Chen, R. Qiang, F. Capolino, and A. A. Oliner, "The role of leaky plasmon waves in the directive beaming of light through a subwavelength aperture", Opt. Expr. **16**, 21271 (2008).
[48] J. J. Burke, G. I. Stegeman, T. Tamir, "Surface-polariton-like guided by thin, lossy metal films", Phys. Rev. B **33**, 5186 (1986).